Appl Magn Reson (2012) 43:139–146
DOI 10.1007/s00723-012-0351-8

Applied
Magnetic Resonance

Liquid State DNP on Metabolites at 260 GHz EPR/400 MHz NMR Frequency

Jan G. Krummenacker · Vasyl P. Denysenkov · Thomas F. Prisner

Received: 28 February 2012 / Revised: 25 April 2012 / Published online: 19 May 2012

Abstract We have performed liquid state ("Overhauser") dynamic nuclear polarization (DNP) experiments at high magnetic field (9.2 T, corresponding to 260 GHz EPR and 400 MHz ^{1}H-NMR resonance frequency) on solutions of pyruvate, lactate and alanine in water with TEMPOL nitroxide radicals as polarizing agent. We present experimental results showing DNP enhancement on metabolite methyl protons, varying for the different target metabolites. It is shown that the enhancements are achieved through direct coupling between the radicals and the target metabolites in solution, i.e., the effect is not mediated by the solvent water protons. The coupling factors between the TEMPOL radicals and the metabolites observed are a factor of 3–5 smaller compared to direct polarization transfer from TEMPOL to water protons.

1 Introduction

Dynamic nuclear polarization (DNP) is a powerful and important technique of enhancing nuclear magnetic resonance (NMR) signals by means of irradiating electron spin transitions of stable radicals in the sample [1–3]. Unfortunately, DNP efficiency drops with increasing field and its implementation becomes technically more challenging. However, high magnetic fields are needed for modern NMR applications for resolution and sensitivity reasons. At high magnetic fields, the pioneering work has been performed in the solid state [4, 5] sparking a surge of new developments and applications [6–9]. This success triggered attempts to investigate also the potential of DNP in the liquid state at high magnetic fields, e.g., at 3.4 T [10–13] and 9.2 T [14–16]. In the liquid state, cross-relaxation between the electron

J. G. Krummenacker · V. P. Denysenkov · T. F. Prisner (✉)
Institute of Physical and Theoretical Chemistry, Center of Biomolecular Magnetic Resonance, Goethe University Frankfurt, Max-von-Laue-Str. 7, 60438 Frankfurt, Germany
e-mail: prisner@chemie.uni-frankfurt.de

and nuclear spin drive the polarization transfer, called Overhauser DNP. Because of the high dielectric losses of most liquid solvents at high microwave frequencies, high-field liquid-state DNP is limited to small sample sizes to avoid excessive microwave heating of the sample. This particularly holds for water as solvent, i.e., for biological samples. Due to the small sample volumes and low filling factors liquid state DNP experiments at high field have so far been limited to studying the polarization transfer to solvent nuclei and not to dissolved molecules. For example, water protons have a concentration of 110 mol/l, while the methyl protons of pyruvate in 1 M solution add up to only 3 mol/l. So in this case, the corresponding ^{1}H-NMR signal is less than 3% of the water proton signal from the solvent making the experiment more demanding. Nevertheless, these experiments are important to understand the polarization transfer mechanism and efficiencies of Overhauser DNP at high magnetic field and to evaluate potential applications in metabolic or biomolecular research.

The Overhauser enhancement factor can be written as

$$\varepsilon_{\mathrm{OE}} = \frac{\gamma_{\mathrm{e}}}{\gamma_{\mathrm{n}}} \times f \times s \times \xi, \tag{1}$$

where γ_e and γ_n are the gyromagnetic ratios of the electron and the nucleus, respectively; i.e. $\frac{\gamma_{\mathrm{e}}}{\gamma_{\mathrm{n}}} \approx -660$ for protons [17].

$f = 1 - \frac{T_{1R}}{T_{1W}}$ is the leakage factor, which can be determined from the nuclear T_1 in the presence ($T_{1\mathrm{R}}$) and in absence of radicals in the solution ($T_{1\mathrm{W}}$).

The factor s denotes the saturation factor, which describes how well the electron transition is saturated by the microwave irradiation. It ranges from 0 for no saturation, i.e., thermal population, to 1 for a fully saturated electron spin transition with equalized populations. At high magnetic field, a full saturation cannot be easily achieved for nitroxide radicals with a large nitrogen hyperfine coupling and very short electron spin relaxation times in liquid solutions. Additionally it is difficult to extrapolate to $s = 1$ from experimental data by a power curve, due to heating of the sample by the microwave irradiation.

ξ is called the coupling factor. It describes how strong the electron and nuclear spins interact with each other. For a magnetic dipole–dipole coupling, which is usually the case for separate radical and target molecules, the coupling factor ranges between 0 and 0.5.

Overall, this yields a maximal theoretical enhancement ($\xi = \frac{1}{2}$, $s = f = 1$) of -330.

2 Experimental

The DNP setup consists of a commercial 400 MHz NMR console (Bruker Avance), equipped with a homebuilt microwave bridge operating at 260 GHz for EPR excitation and detection and a home built double resonance DNP probe (260 GHz/400 MHz) [18].

The DNP probe we used consists of a helix coil for NMR detection, which serves as the body of a TE_{011} cylindrical resonator for the EPR excitation at the same time.

It contains the double resonance structure, radio-frequency (RF) tuning setup, and the metal-dielectric microwave waveguide. The leads of the coil are connected to the RF circuit tuned to 400 MHz NMR frequency. The microwave resonance mode is maintained inside of the helix between two KEL-F plungers with silver coated caps. The structure is coupled to the waveguide in the middle of the helix through an elliptical iris (0.4 by 0.25 mm) in the copper tape of the helix. For microwave cavity tuning, one of the plungers can be moved from outside of the probe via gears and a driving rod. The radio frequency of the NMR circuit can be tuned in the range from 390 to 400 MHz; its conversion factor is 0.17 $mT/W^{1/2}$ and its quality factor Q about 70. The microwave resonance of the cavity can be tuned between 256 and 260 GHz, typically reaching a conversion factor of 0.45 $mT/W^{1/2}$ and a quality factor of approximately 400 [14].

For DNP measurements, the liquid sample is put into a quartz capillary with 50 μm inner diameter (Polymicro TSP050150), which is sealed with wax on both ends and placed along the axis of the cylindrical cavity. With a cavity length of 1.6 mm this yields 4 nl of sample volume.

For typical NMR experiments not requiring a double resonance structure, such as T_{1n} measurements or presaturation experiments, a commercial 400 MHz liquid-state probehead was used (Bruker BBI).

For the irradiation of the electron transitions at 260 GHz, a solid state source (Virginia Diodes), with approximately 45 mW microwave power, was used. It exhibits a frequency instability below 10^{-5}/h and can therefore be used also for prolonged DNP experiments.

Experiments were performed on H_2O/D_2O solutions of (sodium) pyruvate, (sodium) lactate and alanine at 1 M concentrations. These molecules range from 89 to 112 Dalton and exhibit good water solubility, which makes it possible to reach 1 M concentration without any aggregation. Furthermore, these compounds are temperature stable and can withstand the sample heating caused by microwave irradiation during a DNP experiment.

^{14}N-TEMPOL radicals served as polarization agents at a concentration of 12 mM. This radical is well studied and is temperature stable as well.

The enhancements achieved were determined by taking the integrated ^{1}H-NMR line intensities of the samples with and without microwave irradiation of the central hyperfine line of the ^{14}N-TEMPOL radicals, respectively. The spectra were taken using 8192 scans for averaging, to be able to observe the signal from the methyl group of the metabolites.

3 Results and Discussion

Using the helix/cylindrical double-resonance probe and the solid state microwave source with 45 mW power, DNP experiments were performed on three target molecules, all of which are metabolites: Na-pyruvate, Na-lactate or alanine (Fig. 1) were each dissolved in three different solvents; either pure water, 99.9 % deuterated water or partially deuterated water with roughly 3 M water proton concentration, i.e., comparable to the methyl proton concentration of the metabolites. These

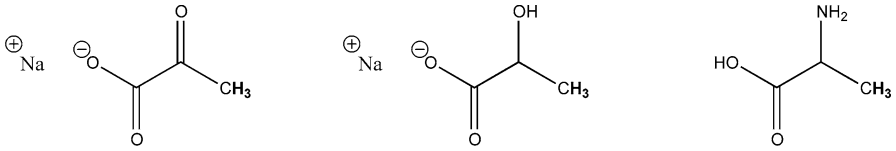

Fig. 1 Chemical structures of the target molecules used in this study. The methyl protons were observed in the DNP experiments

molecules are of general interest as DNP targets because of their use in hyperpolarized metabolic imaging experiments [9, 19]. Because of this, their size and their ease of handling they are ideal for our investigation of liquid DNP polarization transfer to small target molecules in solution.

The enhancement observed on the water protons in these mixtures is comparable to the enhancements achieved for TEMPOL in pure water. The absolute enhancements are rather small because of the low microwave power used, which does not allow saturation of the electron spin transition. Additionally, an enhancement can be observed on the signals from the methyl group on the metabolite, as shown for pyruvate in Fig. 2.

Figure 3 shows the DNP effect for 45 mW microwave power on the methyl protons of pyruvate in protonated water (left), partially deuterated (middle) and 99.9 % deuterated water (right). As can be seen, the enhancement on the methyl protons of pyruvate is effectively unchanged. This proves experimentally that the enhancement on the methyl protons of pyruvate is not mediated by hyperpolarized water protons.

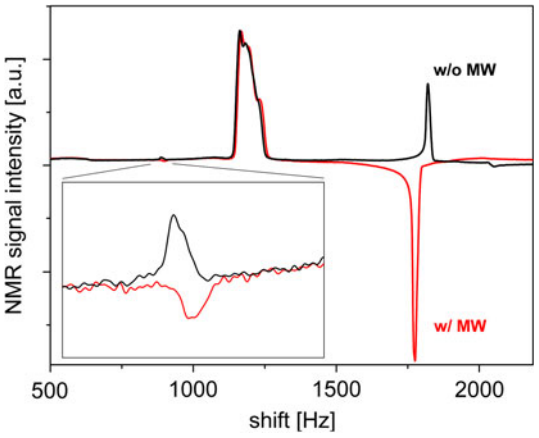

Fig. 2 ^{1}H-NMR spectra of 1 M (sodium) pyruvate solution in water containing 12 mM TEMPOL radical with (*red*) and without microwave irradiation (*black*), respectively. The *inlay* shows enlarged the NMR signal of the CH_3 protons of the pyruvate (*line* at 900 Hz shift), the enhancement factor being −1.6. The enhancement of the water protons (*peak* at 1,600 Hz shift) is −3.9, similar to results with pure water-TEMPOL solutions. The spectra were obtained using 8192 scans. The temperature of the sample inside the resonator is approximately 15 °C above room temperature during microwave irradiation. The large unchanged *peak* at 1,200 Hz shift is due to water outside of the DNP resonator (color figure online)

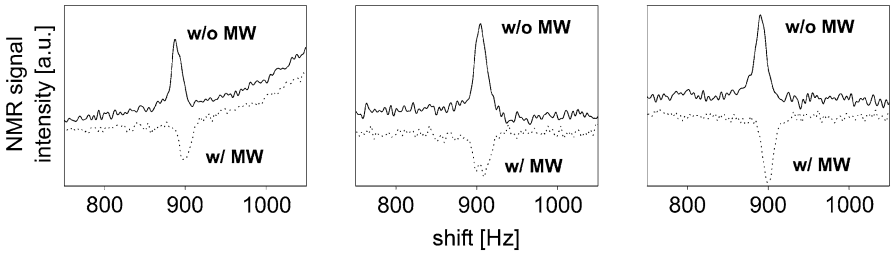

Fig. 3 ^{1}H-NMR spectra of the CH_3 protons of 1 M (sodium) pyruvate solution in protonated water (*left*), partially deuterated water (*middle*) and 99.9 % deuterated water (*right*), containing 12 mM TEMPOL radical with (*dotted*) and without microwave irradiation (*solid line*), respectively. The spectra were obtained using 8192 scans. The achieved enhancement is practically unchanged: −1.6 for water (*left*), −1.5 for partially deuterated water (*middle*) and −1.7 for 99.9 % deuterated water (*right*)

This point is reinforced by performing an experiment, where the water proton peak is diminished by a 20 s presaturation pulse before recording the NMR spectrum and comparing it to the spectrum without the presaturation pulse: while the water proton peak is significantly diminished by the presaturation pulse, the methyl proton peak of pyruvate remains effectively unchanged (Fig. 4).

In conclusion, the enhancement on the methyl protons is not mediated by the water protons, but stems from direct dipolar coupling of the methyl protons to the electron spins. While another pathway of polarization transfer via the solvent protons is imaginable (Fig. 5), it is apparently inactive. This finding is concordant with results at lower magnetic field, where direct ^{13}C polarization on small organic molecules without mediation via abundant proton spins was observed [20].

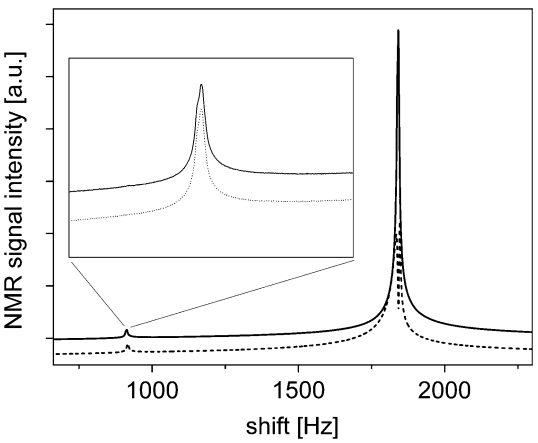

Fig. 4 ^{1}H-NMR spectra of the CH_3 protons of 1 M pyruvate solution in H_2O containing 12 mM TEMPOL radical with and without a 20 s presaturation pulse at the water proton resonance frequency, respectively. The *inlay* shows the pyruvate CH_3 *peak*. While the water *peak* is significantly suppressed, the magnitude of the CH_3 *peak* is effectively unchanged. The spectra were obtained using 16 scans

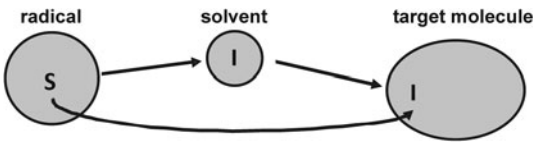

Fig. 5 Possible polarization transfer pathways between radical and target molecule

Table 1 The DNP enhancements on the CH_3 protons of three target metabolites pyruvate, alanine and lactate (left column) and the respective coupling factor ratios to water protons (right column)

Target metabolites	$\varepsilon(CH_3)$	$\xi(H_2O)/\xi(CH_3)$
Pyruvate	-1.6 ± 0.1	2.4 ± 0.2
Alanine	-0.7 ± 0.1	5.3 ± 0.8
Lactate	-1.0 ± 0.1	3.5 ± 0.4

For such a direct coupling, one can basically treat both the water protons and the methyl protons on the metabolite using Eq. 1: the gyromagnetic ratios are the same for both systems, so is the saturation factor s, since it is one and the same experiment. The leakage factor can be determined individually for both kinds of protons by determining their respective T_1 values with and without radicals in an inversion recovery experiment. The leakage factor is practically unaffected by the deuteration of the solvent, e.g., for the pyruvate methyl protons $f = 0.925 \pm 0.028$ for all three solvents. By setting up Eq. 1 for both kinds of protons and dividing the two, the unknown (and hard to access) saturation factor s cancels out and the ratio of the coupling factors of the individual protons can be obtained:

$$\frac{\varepsilon_{OE,H_2O} \times f_{CH_3}}{\varepsilon_{OE,CH_3} \times f_{H_2O}} = \frac{\xi_{H_2O}}{\xi_{CH_3}}.$$

The DNP enhancements on the CH_3 protons of three target metabolites and the respective coupling factor ratios are depicted in Table 1.

The coupling factor is related to the correlation time of the molecular motion via the spectral densities [17].

For a simple hard-sphere model, the correlation time can be calculated using the diffusion coefficients of the electronic (D_S) and the nuclear spin (D_I), respectively, and the distance of closest approach d [17, 21]:

$$\tau = \frac{d^2}{D_S + D_I}.$$

Because the coupling factor decays with $\propto \tau^{-3/2}$ at high magnetic field [22], the theoretically expected ratio of coupling factors can also be obtained from the diffusion coefficients, assuming the same distance of closest approach for both target molecules:

$$\frac{\xi_{H_2O}}{\xi_{CH_3}} = \left(\frac{\tau_{H_2O}}{\tau_{CH_3}}\right)^{-3/2} = \left(\frac{D_S + D_{H_2O}}{D_S + D_{CH_3}}\right)^{3/2}$$

With the room temperature diffusion coefficient for water $D_{H_2O} = 2.3 \times 10^{-9}\,m^2/s$ [23], for the pyruvate ion $D_{CH_3} = 0.44 \times 10^{-9}\,m^2/s$ [24], and using the diffusion coefficient of 4-oxo-TEMPO for the TEMPOL $D_s = 0.41 \times 10^{-9}$ m^2/s [25], a coupling factor ratio of 5.7 is calculated, compared to an experimental value of 2.4. Performing this calculation with a decay of $\propto \tau^{-2}$ [26] renders a coupling factor ratio of 10.2. Due to the sample heating under microwave irradiation, our sample temperature is approximately 40 °C, 15 °C above room

temperature. While the diffusion constants increase with higher temperature, they are assumed to scale with the solvent diffusion constant. In consequence, the obtained ratio of coupling factors can again be compared. In other words, the measured coupling between the pyruvate methyl protons and the electron spin of TEMPOL is stronger than expected theoretically from the diffusion coefficients, using this approach. This might show that local dynamics of the DNP agents/target system play an important role for the DNP enhancement at high magnetic fields [22].

In conclusion, we have performed ^{1}H-DNP experiments on molecules in solution at high magnetic field for the first time. We could show that the DNP enhancements that were observed on the methyl protons of these molecules result from their direct (dipolar) coupling to the radicals and are independent of the solvent proton polarization. Using this, the ratio of the respective high-field coupling factors between water protons and the methyl protons of the metabolites were extracted. They vary by a factor of 2 for the different metabolites and differ approximately a factor of 2 for the pyruvate/TEMPOL sample from theoretical predictions based on translational diffusion. Further work to investigate the dependence of the coupling factor on the specific nature of the DNP agent/target system at high magnetic fields is under way.

Acknowledgments This work was supported by the DIP program from the German Research Council (DFG) and the Center for Biomolecular Magnetic Resonance, Frankfurt. We gratefully acknowledge technical support from Dr. A. Krahn and Dr. F. Engelke from Bruker, Bernhard Thiem and the mechanical workshop of the Institute of Physical Chemistry.

References

1. A.W. Overhauser, Phys. Rev. **92**, 411–415 (1953)
2. T.R. Carver, C.P. Slichter, Phys. Rev. **92**, 212–213 (1953)
3. T.R. Carver, C.P. Slichter, Phys. Rev. **102**, 975–980 (1956)
4. L.R. Becerra, G.J. Gerfen, R.J. Temkin, D.J. Singel, R.G. Griffin, Phys. Rev. Lett. **71**, 3561–3564 (1993)
5. J.H. Ardenkjaer-Larsen, B. Fridlund, A. Gram, G. Hansson, L. Hansson, M.H. Lerche, R. Servin, M. Thaning, K. Golman, Proc. Natl. Acad. Sci. USA **100**, 10158–10163 (2003)
6. K. Golman, R.I. Zandt, M. Lerche, R. Pehrson, J.H. Ardenkjaer-Larsen, Cancer Res. **66**, 10855–10860 (2006)
7. C. Song, K.-N. Hu, C.-G. Joo, T.M. Swager, R.G. Griffin, J. Am. Chem. Soc. **128**, 11385–11390 (2006)
8. M. Reese, D. Lennartz, T. Marquardsen, P. Höfer, A. Tavernier, P. Carl, T. Schippmann, M. Bennati, T. Carlomagno, F. Engelke, C. Griesinger, Appl. Magn. Reson. **34**, 301–311 (2008)
9. S. Hu, M. Zhu, H.A.I. Yoshihara, D.M. Wilson, K.R. Keshari, P. Shin, G. Reed, C. von Morze, R. Bok, P.E.Z. Larson, J. Kurhanewicz, D.B. Vigneron, Magn. Reson. Imaging **29**, 1035–1040 (2011)
10. P.J.M. van Bentum, G.H.A. van der Heijden, J.A. Villanueva-Garibay, A.P.M. Kentgens, Phys. Chem. Chem. Phys. **13**, 17831–17840 (2011)
11. E.V. Kryukov, K.J. Pike, T.K.Y. Tam, M.E. Newton, M.E. Smith, R. Dupree, Phys. Chem. Chem. Phys. **13**, 4372–4380 (2011)
12. P. Höfer, G. Parigi, C. Luchinat, P. Carl, G. Guthausen, M. Reese, T. Carlomagno, C. Griesinger, M. Bennati, J. Am. Chem. Soc. **130**, 3254–3255 (2008)
13. M.-T. Turke, I. Tkach, M. Reese, P. Hofer, M. Bennati, Phys. Chem. Chem. Phys. **12**, 5893–5901 (2010)

14. V. Denysenkov, M.J. Prandolini, M. Gafurov, D. Sezer, B. Endeward, T.F. Prisner, Phys. Chem. Chem. Phys. **12**, 5786–5790 (2010)
15. M.J. Prandolini, V.P. Denysenkov, M. Gafurov, B. Endeward, T.F. Prisner, J. Am. Chem. Soc. **131**, 6090–6092 (2009)
16. M.J. Prandolini, V.P. Denysenkov, M. Gafurov, S. Lyubenova, B. Endeward, M. Bennati, T.F. Prisner, Appl. Magn. Reson. **34**, 399–407 (2008)
17. K.H. Hausser, D. Stehlik, Adv. Magn. Reson. **3**, 79–139 (1968)
18. V.P. Denysenkov, M.J. Prandolini, A. Krahn, M. Gafurov, B. Endeward, T.F. Prisner, Appl. Magn. Reson. **34**, 289–299 (2008)
19. M. Marjańska, I. Iltis, A.A. Shestov, D.K. Deelchand, C. Nelson, K. Uğurbil, P.-G. Henry, J. Magn. Reson. **206**, 210–218 (2010)
20. K. Tsai, H. Dorn, Appl. Magn. Reson. **1**, 231–254 (1990)
21. J.H. Freed, J. Chem. Phys. **68**, 4034–4037 (1978)
22. D. Sezer, M.J. Prandolini, T.F. Prisner, Phys. Chem. Chem. Phys. **11**, 6626–6637 (2009)
23. K.-H. Herrmann, A. Pohlmeier, D. Gembris, H. Vereecken, J. Hydrol. **267**, 244–257 (2002)
24. P. Delahay, J. Am. Chem. Soc. **74**, 3506–3508 (1952)
25. B.D. Armstrong, S. Han, J. Am. Chem. Soc. **131**, 4641–4647 (2009)
26. Y. Ayant, E. Belorizky, J. Aluzon, J. Gallice, J. Phys. France **36**, 991–1004 (1975)